JOURNAL OF VIROLOGY, Dec. 1999, p. 10387–10398 Vol. 73, No. 12
0022-538X/99/$04.00+0

Infection of Neonatal Mice with Sindbis Virus Results in a Systemic Inflammatory Response Syndrome

W. B. KLIMSTRA,[1]* K. D. RYMAN,[1] K. A. BERNARD,[1] K. B. NGUYEN,[2] C. A. BIRON,[2] AND R. E. JOHNSTON[1]

Department of Microbiology and Immunology, University of North Carolina at Chapel Hill School of Medicine, Chapel Hill, NC 27599-7290,[1] and Department of Molecular Microbiology and Immunology, Division of Biology and Medicine, Brown University, Providence, Rhode Island 02912[2]

Received 26 May 1999/Accepted 7 September 1999

Laboratory strains of viruses may contain cell culture-adaptive mutations which result in significant quantitative and qualitative alterations in pathogenesis compared to natural virus isolates. This report suggests that this is the case with Sindbis virus strain AR339. A cDNA clone comprising a consensus sequence of Sindbis virus strain AR339 has been constructed (W. B. Klimstra, K. D. Ryman, and R. E. Johnston, J. Virol. 72:7357–7366, 1998). This clone (pTR339) regenerates a sequence predicted to be very close to that of the original AR339 isolate by eliminating several cell culture-adaptive mutations present in individual laboratory strains of the virus (K. L. McKnight et al., J. Virol. 70:1981–1989, 1996). It thus provides a unique reagent for study of the pathogenesis of Sindbis virus strain AR339 in mice. Neonatal mouse pathogenesis of virus (TR339) generated from the pTR339 clone was compared with that of virus from a cDNA clone of the cell culture-passaged laboratory AR339 strain, TRSB, and virus from a clone of a more highly cell culture-adapted strain, HR_{sp} (Toto 50). The sequence of TRSB differs from the consensus at three coding positions, while Toto 50 differs at eight codons and one nucleotide in the 5′ nontranslated region. Both cell culture-adapted strains contain mutations associated with heparan sulfate (HS)-dependent attachment to cells (W. B. Klimstra, K. D. Ryman, and R. E. Johnston, J. Virol. 72:7357–7366, 1998). TR339 caused 100% mortality with an average survival time (AST) of 1.7 ± 0.25 days. While TRSB also caused 100% mortality, the AST was extended to 2.9 ± 0.52 days. The more extensively cell culture-adapted virus Toto 50 caused only 30% mortality with an AST extended to 11.0 ± 4.8 days. TRSB and TR339 induced high serum levels of alpha/beta interferon, gamma interferon, tumor necrosis factor alpha, interleukin-6, and corticosterone and induced pathology reminiscent of lipopolysaccharide-induced endotoxic shock, a type of systemic inflammatory response syndrome. However, the reduced intensity of this response in TRSB-infected mice correlated with the increased AST. Toto 50 failed to induce the shock-like cytokine cascade. In situ hybridization studies indicated that TR339 and TRSB replicated in identical tissues, but the TRSB signal was less widespread at early times postinfection. While Toto 50 also replicated in similar tissues, the extent of replication was severely restricted and mice developed lesions characteristic of encephalitis. A single mutation in TRSB at E2 position 1 (Arg) conferred HS-dependent attachment to cells and was associated with reduced cytokine induction and extended AST in vivo.

Sindbis virus, the prototype member of the *Alphavirus* genus, is a positive-sense RNA virus with a genome of 11,703 nucleotides (55). Sindbis virus strain AR339, originally isolated in 1952 in Sindbis, Egypt (57), has been used extensively in in vitro studies of the alphavirus life cycle and in studies of its pathogenesis in mice (28, 40, 51, 61). Virtually all of these studies have employed either biological strains derived after passage of Sindbis virus strain AR339 in cultured cells or virus derived from cDNA clones of such passaged viruses (31).

Some laboratory isolates of Sindbis virus strain AR339 cause a rapidly fatal disease in neonatal mice inoculated subcutaneously (s.c.) or intracerebrally (52, 57, 61). With the s.c. route of infection, virus replication is first observed in skeletal muscle, skin, and fibroblast-connective tissue, with virus becoming disseminated throughout the animal by 24 h postinfection (hpi) (14, 61). This early replication leads to virus invasion of the central nervous system and infection of neurons (14, 51, 61). Mortality has been ascribed to fatal encephalitis (14, 51). However, pathology studies have shown little evidence of T- or B-cell-mediated disease with Sindbis virus (14, 15, 29, 61), and neonatal immunodeficient *scid* mice also succumb to fatal disease (24). Neonatal mice infected intracerebrally with virus constructs expressing inhibitors of apoptosis exhibit reduced mortality (23, 35), suggesting a direct effect of virus replication in neurons on disease outcome. In studies of other laboratory strains, however, overwhelming virus replication and damage in extraneural tissues have been implicated in the induction of a potentially toxic inflammatory cytokine and stress mediator cascade which is associated with neonatal mouse mortality but occurs in the absence of frank encephalitis (61, 63). Therefore, a number of factors may contribute to Sindbis virus-induced mortality, depending upon the virus strain used, the route of inoculation, and the age of the mouse at the time of infection (51, 61, 63, 64).

A difficulty in interpreting these studies is that even virulent laboratory isolates of Sindbis virus strain AR339 that cause 100% mortality contain mutations associated with attenuation of disease in mice (31). Comparisons of laboratory viruses with more extensively cell-adapted strains have resulted in the identification of several loci in the structural glycoproteins and at least one in the 5′ nontranslated region (NTR) that can influence neonatal mouse virulence (28, 31, 40, 51, 61). One class of cell culture-adaptive mutations in the E2 glycoprotein confers

* Corresponding author. Mailing address: Department of Microbiology and Immunology, University of North Carolina at Chapel Hill School of Medicine, Chapel Hill, NC 27599-7290. Phone: (919) 966-4026. Fax: (919) 962-8103. E-mail: wklimstr@med.unc.edu.

the ability to use heparan sulfate (HS) as a cell attachment receptor (19, 31). Such mutations arise very rapidly during propagation of AR339 in cell culture (19). Therefore, cell culture-adaptive attenuating mutations may well be embedded in low-passage biological or cDNA-cloned laboratory strains considered to be wild type.

TRSB, the low cell passage strain used in this laboratory, does not induce frank encephalitis in neonatal mice. Instead, the disease is characterized by extensive virus replication in extraneural tissues and the induction of high levels of several proinflammatory cytokines and corticosterone (61, 63), suggestive of a systemic inflammatory response syndrome (SIRS) (1, 2, 5). This type of pathogenesis differs significantly from the predominantly encephalitic disease course that has been associated with Sindbis virus infection previously (14, 51). One possible explanation for this difference is that the shock-like syndrome and the lack of encephalitis in TRSB infection are an artifact of cell culture-adaptive mutations unique to this laboratory strain. A second explanation is that because the TRSB sequence is very close to the consensus sequence of AR339, differing by only three mutations, a systemic inflammatory response may be characteristic of the fully virulent manifestations of Sindbis virus infection, while a more encephalitic pathogenesis is associated with attenuated laboratory strains.

To test these alternative explanations, we have constructed a cDNA clone comprised of the consensus sequence of Sindbis virus strain AR339 (19, 31). Virus generated from this clone, pTR339, which purges the sequence of several known cell culture-adaptive mutations present in laboratory isolates of Sindbis virus strain AR339, does not rely on HS attachment for cell infection and is likely closer in sequence to the original Sindbis virus strain AR339 isolate than are any of the laboratory strains (31). In the studies reported here, we have compared the pathogenesis of TR339 in neonatal mice with the pathogenesis of TRSB and a more highly cell culture-adapted strain, HR_{sp} (cDNA clone Toto 50). While these viruses replicated in identical tissues, increased mortality and decreased survival time were correlated with higher levels of virus replication and the increased magnitude of induction of proinflammatory cytokines, such as alpha/beta interferon (IFN-α/β), tumor necrosis factor alpha (TNF-α), gamma interferon (IFN-γ), and interleukin-6 (IL-6), as well as systemic stress response mediators. These findings strongly suggest (i) that the TR339-infected mice had SIRS, (ii) that the SIRS response in the absence of frank encephalitis contributes significantly to the pathogenesis of fully virulent Sindbis virus strain AR339 in neonatal mice, and (iii) that cell culture-adaptive mutations conferring HS attachment contribute to the attenuation of Sindbis virus laboratory strains.

MATERIALS AND METHODS

Viruses. Construction of the cDNA clones of the biological laboratory strain, pTRSB, and the AR339 consensus sequence virus, pTR339, has been previously described (19, 31). The "p" prefix refers to the plasmid form of the cloned virus. The three coding differences present in pTR339, compared with pTRSB (Table 1), were introduced individually into the pTRSB background by restriction endonuclease fragment exchange from pTR339. Arginine at nsP3 position 528 was obtained from a *Spe*I-to-*Hpa*I fragment (clone designated pnsP3 528); serine at E2 position 1 was obtained from a *Stu*I-*Bss*HII fragment (clone designated pE2S1); and alanine at E1 position 72 was obtained from a *Bss*HII-to-*Xho*I fragment (clone designated pE1 72). pToto 50, a cDNA clone of the HR_{sp} strain of AR339 (43), was a gift from Charles Rice, Washington University, St. Louis, Mo. All genetic manipulations were confirmed by DNA cycle sequencing (USB). Virus stocks were generated by in vitro transcription of linearized cDNA templates, followed by electroporation of the transcripts into BHK-21 cells (American Type Culture Collection; maintained in alpha minimum essential medium [GIBCO] supplemented with 10% donor calf serum, 10% tryptose phosphate broth, L-glutamine, 100 U of penicillin per ml, and 0.05 mg of streptomycin per ml). Electroporation supernatants were harvested after 18 to 20 h, clarified, and stored at −70°C. Titers of electroporation stocks were determined by standard plaque assay on BHK cells, and the stocks were used directly for mouse infection.

TABLE 1. Amino acid differences and binding phenotypes of viruses used in pathogenesis studies

Virus[a]	nsP3 528	E2 1	E1 72	Mean binding[b] ± SD	Mean specific infectivity[c] ± SD
TR339	Arg	Ser	Ala	7.4 ± 1.1	5.6 ± 0.2
TRSB	Gln	Arg	Val	100.0 ± 16.1	100.0 ± 15.9
nsP3 528	Arg	Arg	Val	131.6 ± 31.8	118.4 ± 18.1
E2S1	Gln	Ser	Val	8.0 ± 4.0	6.6 ± 1.1
E1 72	Gln	Arg	Ala	89.5 ± 15.4	68.3 ± 3.74
Toto 50[d]	Arg	Ser	Ala	372.8 ± 81.9	539.3 ± 86.3

[a] Viruses other than Toto 50 are isogenic except for the indicated loci.
[b] Relative binding to BHK cells; all values are normalized to TRSB = 100.
[c] Relative numbers of BHK cell PFU per count per minute of radiolabeled virus; all values are normalized to TRSB = 100.
[d] Toto 50 differs from the consensus sequence at eight coding positions and nucleotide 5 of the 5′ NTR.

Mice. Pregnant outbred CD-1 females (13 to 15 or 15 to 17 days of gestation) were obtained from Charles River Laboratories. Mice were infected s.c. with 10^3 PFU of each virus in 50 μl of virus buffer (VB; phosphate-buffered saline–1% donor calf serum) at 12 to 24 h postnatally. Mice were sacrificed at 12-h intervals through 72 hpi for virus titer determination and cytokine assays or observed at 12- or 24-h intervals through day 21 for mortality and average survival time (AST).

Virus attachment and infectivity assays. Radiolabeling ([^{35}S]methionine), purification of virus, and suspension binding assays were performed exactly as previously described (19). This method was previously shown to give results similar to those of cell monolayer binding assays with Sindbis virus (19). For binding assays, BHK cells were dissociated from tissue culture plates using enzyme-free cell dissociation buffer (GIBCO) and washed three times with VB prior to reaction with virus. Fifty-microliter volumes of cells (~10^6) were added to Eppendorf tubes, followed by 50-μl volumes of purified virus (10^5 cpm/reaction mixture), and reaction mixtures were incubated at 4°C for 60 min with gentle agitation. Cells then were washed three times with 1 ml of VB, and radioactivity associated with cells was determined by scintillation counting. Cell-free control reactions were run for each binding experiment, and the counts per minute adherent to reaction tubes were subtracted from the total counts per minute bound. Specific infectivity (number of PFU divided by counts per minute) was calculated as previously described (19). Binding reactions were done in duplicate or triplicate, and all experiments were repeated at least twice.

Virus, cytokine, and corticosterone titrations. Whole blood obtained from mice was separated into serum and erythrocyte fractions by using Microtainer serum separators (Becton-Dickinson). Serum samples were obtained from either individual mice or a pool of 5 to 10 mice. Brains were removed, diluted 1:1 in VB, homogenized, and centrifuged, and the clarified supernatant was aliquoted. All samples were stored at −70°C prior to assay. Virus titers in serum and brain samples were measured by standard plaque assay on BHK cells. The IFN-α/β titer was determined by biological assay as previously described (61). Mouse TNF-α was measured by using the Factor-X ELISA kit (Genzyme). IL-6 and IFN-γ were measured by enzyme-linked immunosorbent assay as previously described (36, 38). Serum corticosterone was measured with a radioimmunoassay kit (ICN).

Histopathology and ISH analysis. After euthanization, the cranial, thoracic, and abdominal cavities of at least two mice per time point were opened and the mice were immersion fixed in a 10% formalin solution (Fisher). Heads and bodies, with the thymuses removed and processed separately, were bisected midsagittally, embedded in paraffin, and then sectioned. Hematoxylin and eosin (H&E)-stained tissues were examined by light microscopy. In situ hybridization (ISH) analysis for sites of virus replication was performed essentially as described by Trgovcich et al. (61). However, a negative control probe derived from the *EBER* gene of Epstein-Barr virus (EBV) was used. Controls consisted of infected-mouse tissues incubated with the EBV probe and uninfected-mouse tissues incubated with the virus-specific probe. Photomicrographs were taken on a Nikon photomicroscope.

LPS treatment. Neonatal mice were injected intraperitoneally with lipopolysaccharide (LPS; *Escherichia coli* 111:226; Sigma) at 30 mg/kg in 20 μl of VB. In preliminary titrations, this dose caused 95 to 100% mortality. LPS- and mock-treated mice were sacrificed at 2, 4, 8, and 20 hpi for serum cytokine (5 to 10 mice, pooled) and histopathological (3 mice per time point) analyses as described above. LPS-treated mice were also sacrificed for assay at 28 hpi.

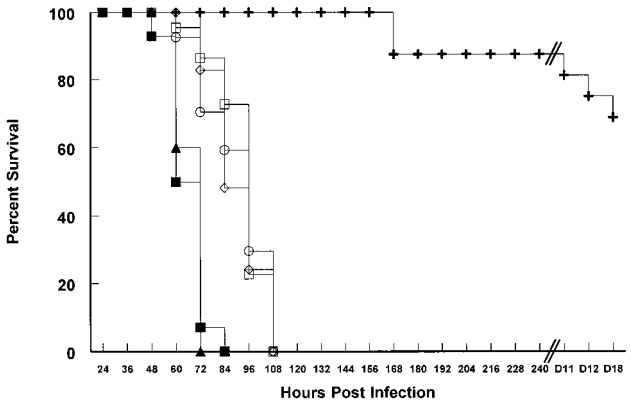

FIG. 1. Survival of neonatal mice infected with TR339 (▲), E2S1 (■), TRSB (□), nsP3 528 (◇), E172 (○), or Toto 50 (+). Mice were infected s.c. with 1,000 PFU of each virus in 50 μl of virus diluent.

RESULTS

Five noncoding and three coding differences distinguish the Sindbis virus AR339 consensus sequence from that of our laboratory strain cDNA clone, pTRSB (31) (Table 1). None of the noncoding differences are located in identified alphavirus *cis*-acting sequences, and they have not been considered as candidate loci affecting pathogenesis. In comparison, the HR_{sp} (biological progenitor of clone Toto 50) sequence differs at eight coding positions and at nucleotide 5 of the 5′ NTR. Four of these loci have been identified previously as affecting AR339 pathogenesis in mice (28, 31). Based on mortality and AST, TR339 is the most virulent of these viruses, followed, in order of decreasing virulence, by TRSB and Toto 50 (19, 51, 61). To evaluate the relative contribution of each of the differences between TRSB and TR339 to the greater virulence of TR339, we have constructed cDNA clones with each TR339 difference residue substituted separately into the TRSB background (Table 1).

Binding to BHK cells. The Ser (TR339)-to-Arg (TRSB) difference at position 1 of the E2 structural glycoprotein confers a significant increase in binding of TRSB to BHK cells, and this binding is dependent upon the presence of cell surface HS (19). Binding studies with viruses differing at the three coding positions that distinguish TRSB and TR339 indicated that only the Ser-to-Arg change at E2 position 1 resulted in a large difference in attachment to BHK cells (Table 1). The specific infectivity of the viruses covaried with binding, suggesting that the relative ability to establish infection of the cells was determined by attachment efficiency (Table 1). The binding and infectivity of Toto 50 were significantly greater than those of the other viruses. Previous studies indicate that this virus also attaches to HS receptors on cultured cells (13, 19). The specific infectivity data suggest that in terms of the numbers of PFU determined on BHK cells, virus particle-to-PFU ratios are very different between these viruses, with Toto 50 < TRSB, nsP3 528, and E1 72 < E2S1 and TR339. TR339 ranged from 20- to 100-fold less infectious per count per minute for BHK cells than TRSB, and Toto 50 was 3- to 5-fold more infectious for BHK cells than was TRSB. This suggests that BHK cell plaque assays significantly underestimate the number of TR339 particles relative to those of TRSB and Toto 50.

TABLE 2. Mortality and AST of neonatal mice infected with the viruses used in the current studies

Virus	No. of mice	Mortality (%)	AST (days)
TR339	30	100	1.7 ± 0.25
E2S1	30	100	1.9 ± 0.53
TRSB	30	100	2.9 ± 0.52
nsP3 528	32	100	2.8 ± 0.55
E1 72	29	100	2.9 ± 0.53
Toto 50	16	31.3	11.0 ± 4.80

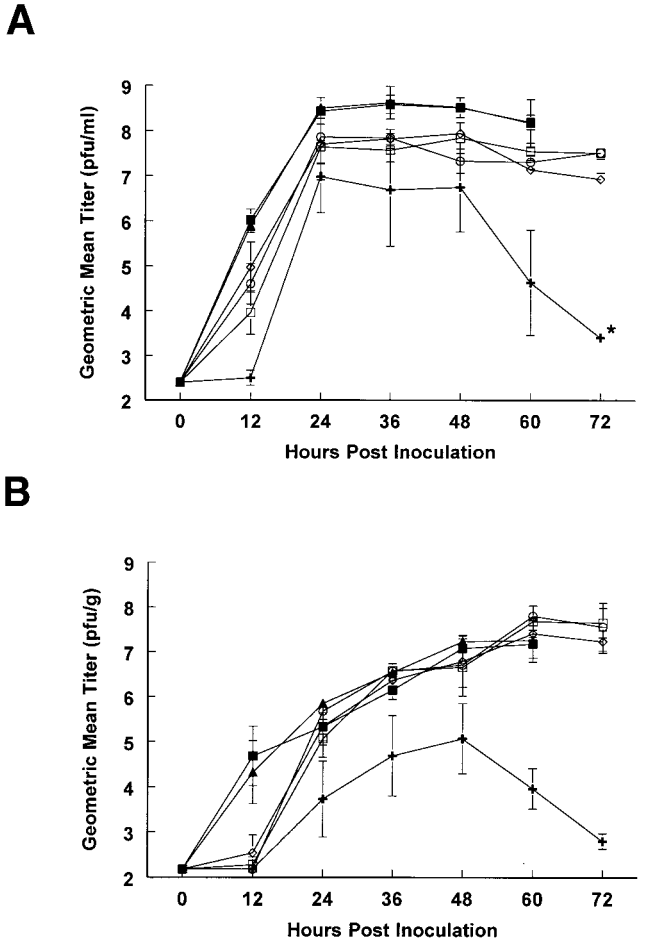

FIG. 2. Titers of virus in sera (A) and brains (B) of infected neonatal mice. Symbols: □, TRSB; ◇, nsP3 528; ○, E1 72; ■, E2S1; ▲, TR339; +, Toto 50; ∗, Toto 50 titer below the limit of detection of the plaque assay (3,500 PFU/ml).

Virulence in neonatal mice. TR339 exhibited increased virulence over the laboratory strain virus TRSB, resulting in very rapid death of all infected mice and a significant reduction in AST (two-tailed Student *t* test, $P < 0.01$) compared with TRSB (Fig. 1 and Table 2). When the three coding differences between TRSB and TR339 were evaluated individually, it was found that substitution of the TR339 Ser for the TRSB Arg at E2 position 1 was sufficient to confer virulence similar to that of TR339 ($P > 0.1$). The residues at nsP3 position 528 and E1 position 72 had no significant effect on virulence ($P > 0.4$). In comparison, Toto 50 showed only ~30% mortality and a greatly extended AST, consistent with previous reports (51).

The differences among TRSB-like viruses, TR339-like viruses, and Toto 50 in specific infectivity for BHK cells (Table 1) indicate that mouse inocula comprised of equal numbers of BHK PFU would contain more TR339-like virus particles. However, in preliminary virus titration experiments, ASTs of

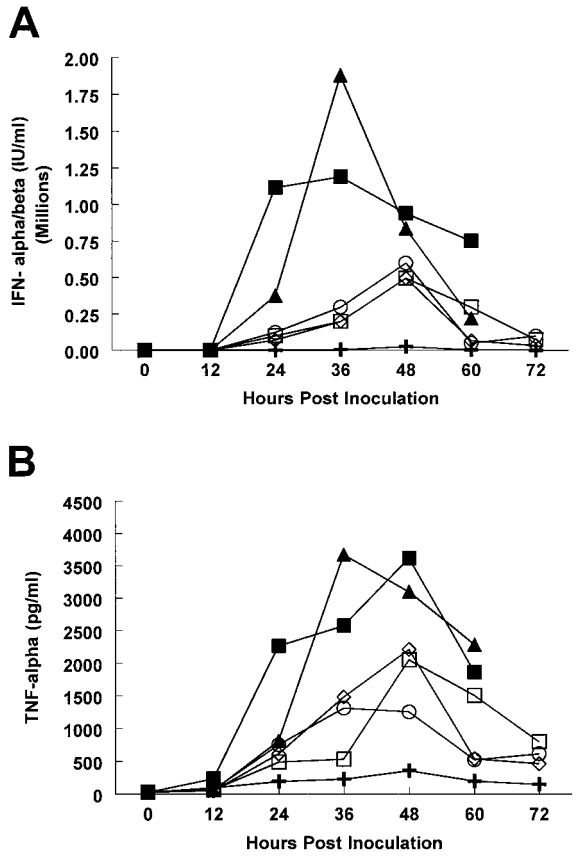

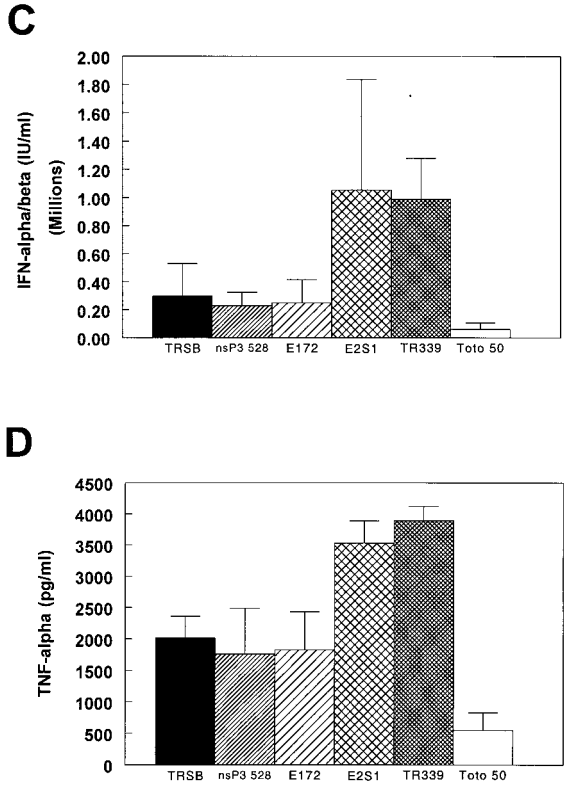

FIG. 3. IFN-α/β and TNF-α levels in pooled and individual sera of infected neonatal mice. Levels in mock-infected animals were below the limits of detection for these assays. (A) IFN-α/β as measured in serum pools from 5 to 10 mice. (B) TNF-α pooled samples (5 to 10 mice). Symbols: □, TRSB; ◇, nsP3 528; ○, E1 72; ■, E2S1; ▲, TR339; +, Toto 50. (C) Peak IFN-α/β levels in sera of individual mice ($n = 3$). (D) Peak TNF-α levels in sera of individual mice ($n = 3$). Levels in mock-infected animals were below the limits of detection for these assays.

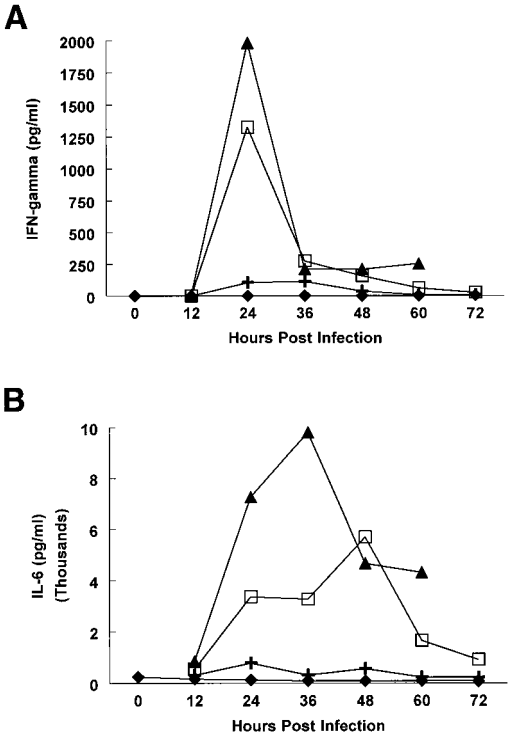

FIG. 4. IFN-γ and IL-6 levels in pooled sera of infected neonatal mice. Samples represent pooled sera from 5 to 10 mice that were mock infected (◆) or infected with TRSB (□), TR339 (▲), or Toto 50 (+).

TR339- and E2S1-infected neonates did not vary significantly when mice were given between 1,000 and 0.01 BHK PFU (data not shown). This indicates that TR339-like viruses are intrinsically more virulent than TRSB-like viruses. Similarly, the AST and percent mortality of TRSB-infected mice did not vary with decreasing dose (data not shown), confirming that Toto 50 particles are intrinsically less virulent regardless of the dose.

Virus replication in neonatal mice. Twelve- to 24-h-old CD-1 mice were infected s.c. with 10^3 PFU of each virus listed in Table 1. Mice were sacrificed at 12-h intervals through 72 hpi, and infectious virus titers in brain suspensions and serum were determined on BHK cells. Consistent with the virulence studies, serum virus titers indicated that TR339 replicated to higher titers at all times postinfection (Fig. 2A) and that substitution of Ser for Arg at E2 position 1 in the TRSB background was sufficient to confer this phenotype. Virus with the TR339 residues at nsP3 position 528 or E1 position 72 in the TRSB background segregated with TRSB, and Toto 50 exhibited lower titers at all times. As indicated by the cell infectivity assays described above, BHK cell plaque assays likely underestimate the numbers of TR339 and E2S1 particles relative to those of TRSB, nsP3 528, and E1 72 and similarly overestimate the number of Toto 50 particles. Adjustment of the titration results for BHK cell infectivity would increase TR339 and E2S1 titers by 15- to 20-fold and decrease Toto 50 titers by 3- to 5-fold. Likewise, while brain BHK cell titers indicated no significant differences between TRSB and TR339 between 24 and 60 hpi, regardless of the residue at nsP3 position 528, E2 position 1, or E1 position 72 (Fig. 2B), adjustment for BHK cell infectivity would indicate higher titers for TR339 and E2S1. A clear lag in brain replication was seen at 12 hpi with TRSB, nsP3 528, and E1 72, and replacing the consensus Ser with Arg at TRSB E2 position 1 was sufficient to overcome the lag. Even without BHK cell infectivity adjustment, Toto 50 brain titers were lowest at all times postinfection.

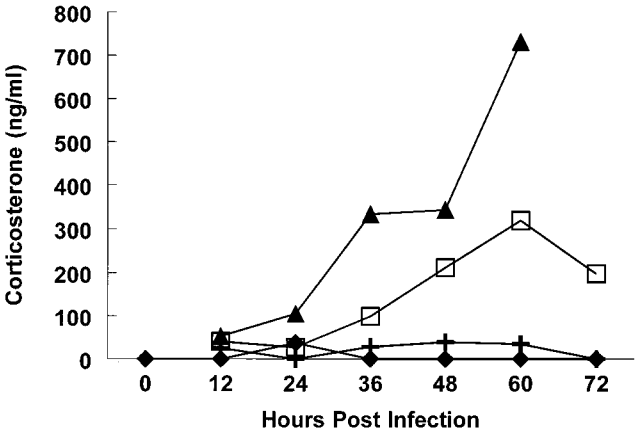

FIG. 5. Corticosterone levels in pooled sera of infected neonatal mice. Samples represent pooled sera from 5 to 10 mice infected with TRSB (□), TR339 (▲), or Toto 50 (+) and mock-infected mice (◆).

Induction of proinflammatory cytokines and stress mediators. In infections of neonatal mice with TRSB and an attenuated mutant, a correlation was established among induction of IFN-α/β, TNF-α, and corticosterone; a high virus titer; and mortality (61, 63). The presence of TNF-α and corticosterone suggested a previously unrecognized SIRS component in Sindbis virus disease. To test whether this pathology was an anomalous manifestation of one of the mutations present in TRSB or whether the consensus sequence virus also was associated with the shock-like syndrome, these parameters, as well as IFN-γ and IL-6, were measured in pooled animal sera at 12-h intervals after infection. In addition, assays were performed on sera of individual mice at 24, 36, and 48 hpi, times determined in preliminary assays to correspond to peak cytokine induction (data not shown). The results shown in Fig. 3 to 5 demonstrate that TR339, comprising the consensus Sindbis virus AR339 sequence, induced an even more severe shock-like response than TRSB and that the greater intensity of this response was correlated with increased virulence.

Induction of IFN-α/β correlated with serum virus titer for all of the viruses tested (Fig. 3A). This is consistent with previous reports of IFN-α/β induction in Sindbis virus-infected mice (e.g., reference 61). Comparing TR339 and TRSB, IFN-α/β induction segregated with the Ser-Arg change at E2 position 1. TR339- and E2S1-infected animals produced severalfold higher IFN-α/β titers at all times postinfection, peaking at nearly 2×10^6 IU/ml. Serum TNF-α levels also were closely correlated with virulence (Fig. 3B). TR339 and E2S1 peak values approached 4,000 pg/ml and were roughly twofold higher than those of TRSB, nsP3 528, and E1 72. Infection with Toto 50 produced low levels of IFN-α/β and TNF-α. For both IFN-α/β and TNF-α, levels in individual mice were generally consistent with those from pooled samples (Fig. 3C and D). TR339 and E2S1 induced peak levels of TNF-α significantly higher than those of TRSB, nsP3 528, and E1 72 ($P \leq 0.02$), and these levels were significantly higher than that of Toto 50 (TRSB, $P < 0.01$; nsP3 528, $P = 0.03$; E1 72, $P < 0.01$). Levels of TNF-α similar to those for TRSB and TR339 have been associated with a fatal outcome in LPS-treated adult mice and in models of bacterial sepsis (4, 25, 50, 59), and high levels of IFN-α/β cause liver, spleen, and thymus pathology in neonatal mice (9).

Since measures of virulence such as AST, virus titer, and induction of IFN-α/β and TNF-α segregate with the Ser-to-Arg substitution at E2 position 1, one representative of each group (TRSB or TR339) was analyzed further in combination with Toto 50. The magnitude of IFN-γ and IL-6 induction also correlated with virus virulence (Fig. 4A and B). IFN-γ was produced in a burst at 24 hpi, with levels falling by 36 hpi, perhaps revealing an early effect of stimulation of NK or T cells. IL-6 induction increased during infection to levels approaching 10,000 pg/ml with TR339, almost twofold higher than TRSB-induced levels. Although the kinetics of induction were slightly variable between animals, IFN-γ and IL-6 levels in sera of individual mice were consistent with those in pooled samples (data not shown), with TR339-induced levels significantly higher than TRSB-induced levels ($P = 0.01$ for IFN-γ; $P < 0.01$ for IL-6) and TRSB-induced levels significantly higher than Toto 50-induced levels ($P < 0.01$ for both).

Induction of the systemic stress mediator corticosterone is implicated in a feedback mechanism by which proinflammatory cytokine responses are damped during septic shock, with production of corticosterone potentially mediated through direct action of IL-6 or IL-1β on the hypothalamic-pituitary axis (46, 47, 60). Corticosterone levels in pooled sera from TR339- and TRSB-infected mice increased through 60 hpi, with levels in TR339-infected mice rising earlier and to a higher peak level and reflecting the virulence of the inducing virus (Fig. 5). These results suggest that the proximal stress hormone-inducing factor is closely correlated with virus replication. Pooled samples from Toto 50-infected mice exhibited only mild stress mediator induction with serum levels approximately 10-fold lower than TRSB-induced levels and greater than 20-fold lower than TR339-induced levels.

ISH and histopathological analyses. To determine if any quantitative or qualitative differences in sites or extent of virus replication correlated with virulence differences, tissue sections from TR339-, TRSB-, and Toto 50-infected mice were evaluated by ISH for sites of viral RNA production. H&E-stained sections were observed for pathological changes. Sections from mock-infected animals treated with the Sindbis virus-specific probe and virus-infected animals treated with an EBV-specific probe showed no positive signal other than occasional staining of keratinized skin epithelium (found with all probes and in mock-infected animals), indicating that the ISH signal was specific for sites of Sindbis virus genome expression.

At 12 hpi, a positive punctate ISH signal was seen consistently in skin, periosteum, and skeletal muscle associated with the site of inoculation in TR339-infected mice (data not shown). In addition, an occasional signal was observed in similar tissues distant from the inoculation site. With TRSB, the virus signal was not seen consistently at the inoculation site and was less intense and less widespread when observed. No ISH signal was found at 12 hpi in mice infected with Toto 50, and pathological changes were not observed with any of the viruses at 12 hpi (data not shown).

By 24 hpi, TR339-infected mice exhibited a diffuse positive signal in skeletal muscle and fibroblast-connective tissue throughout the animal, extending into the tail, feet, legs, and head. In addition, a focal signal was observed in the dermis of the skin, brown fat, myocardium, heart valves (Fig. 6A), lungs, liver, kidneys, diaphragm, spleen, and gastrointestinal tract smooth muscle (data not shown). This was accompanied occasionally by infiltration of mononuclear cells in skeletal muscle and the heart. However, at this time, while virus titers could be detected in brains (see above), only rare positive ISH signal foci could be observed (data not shown). As described above, proinflammatory cytokines and stress mediators were induced significantly over the background by 24 hpi, apparently in the absence of significant virus genome expression in the brain.

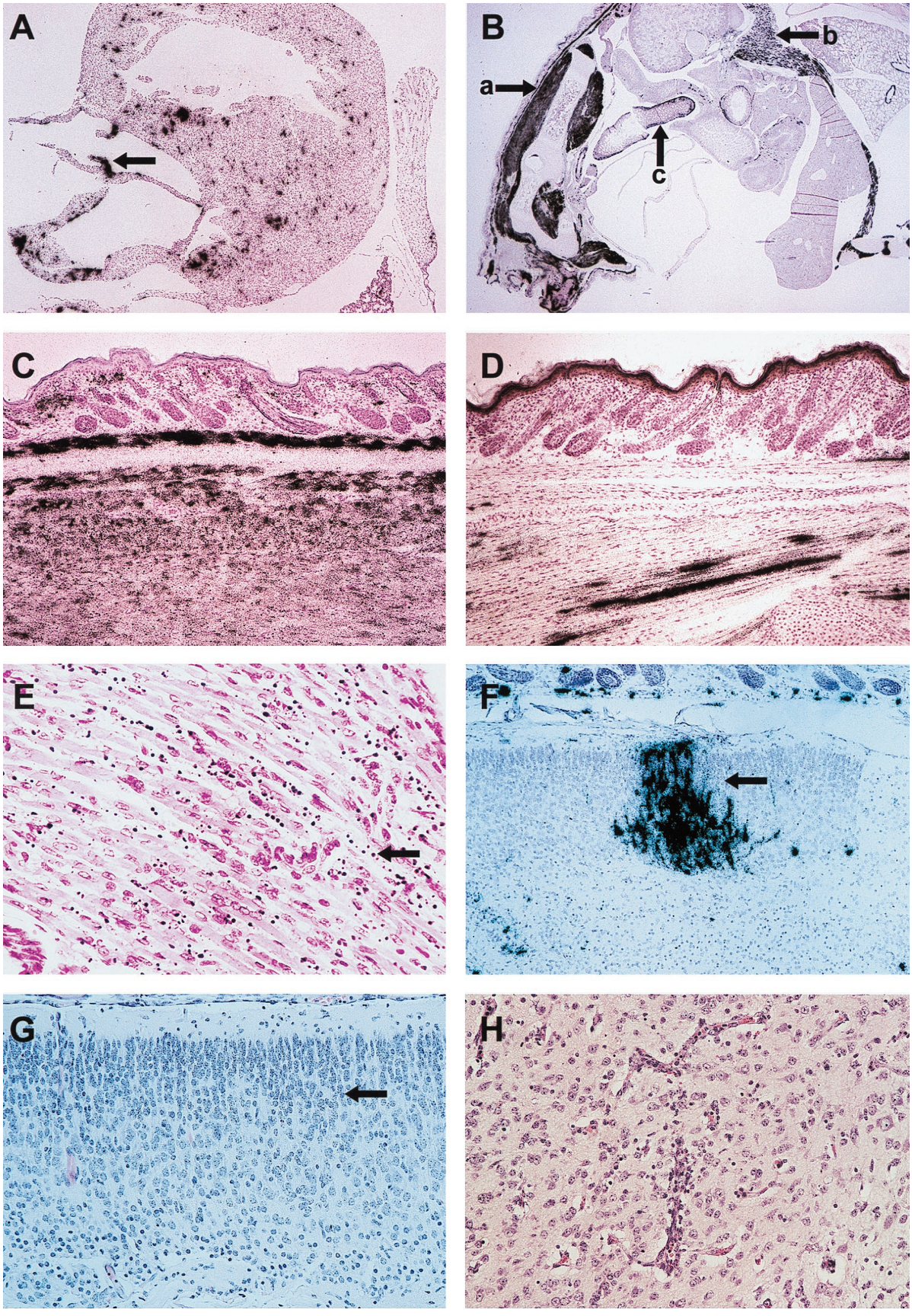

FIG. 6. Histopathological and ISH analyses of virus-infected neonatal mice. (A) ISH showing virus replication in the myocardium and valves (arrow) of the heart at 24 hpi (original magnification, ×40). (B) ISH of the caudal portion of a midsagittal section through the body of a TR339-infected mouse sacrificed at 60 hpi (original magnification, ×10). Arrows indicate virus replication in the skeletal muscle (a), the diaphragm (b), and the muscularis of the gut (c). (C) ISH showing confluent virus replication in skeletal muscle of a TR339-infected mouse at 60 hpi (original magnification, ×100). (D) ISH showing focal replication of Toto 50 at 48 hpi (original

This suggests that virus replication in peripheral tissues is responsible for induction of cytokines measured in serum. TRSB signal was present in virtually identical tissue types and sites; however, the signal was less intense and less widespread. In Toto 50-infected mice, the positive ISH signal was confined to focal sites in skeletal muscle, the lungs, and connective tissue and no signal was observed in the brain (data not shown).

The ISH signal was more widespread in TR339-infected mice prior to 60 hpi, at which time the signal extent was equivalent between TRSB and TR339 (Fig. 6B and C). By 60 hpi, an intense ISH signal was found in virtually all of the skeletal muscle and fibroblast-connective tissue of the animals (Fig. 6B and C). A signal also was observed in the myocardium and heart valves (data not shown), the smooth muscle of the intestinal tract, and the capsular-endothelial tissue of the liver, kidneys, and lungs (Fig. 6B). H&E-stained sections revealed widespread and dramatic necrosis and/or apoptosis of virus-infected skeletal muscle in association with occasional mononuclear cell infiltrates (Fig. 6E). In addition, apoptotic and/or necrotic cells associated with occasional mononuclear cell infiltrates were noted in virus-infected esophageal muscle, lungs, dermis of the skin (Fig. 7B), brown fat, and smooth muscle of the intestinal tract. All types of tissue damage were more common and more severe in TR339-infected animals. Diminution of subcutaneous fat was first observed at 24 hpi and was striking in TRSB- and TR339-infected mice by 48 to 60 hpi, compared to mock- or Toto 50-infected mice (Fig. 7A and B).

In the brain, sites of virus replication were widely distributed at 60 hpi and were associated with cells of neuronal morphology. However, infection was focal (Fig. 6F), in contrast to the nearly complete infection of skeletal muscle and connective tissue in the periphery (Fig. 6B and C), and neither inflammatory changes, morphological signs of severe cellular necrosis or apoptosis, nor extensive mononuclear cell infiltration was apparent with either TR339 or TRSB infection (Fig. 6G). A slight increase in the number of condensed and fragmented cell nuclei was observed in the brains of virus-infected mice late in infection (data not shown). However, similar changes were occasionally seen in mock-infected animals and were also observed in LPS-treated mice (see below). This was in contrast to the severe damage associated with virus replication in the skin, skeletal muscle, and connective tissue (Fig. 6E and 7B). Tissue types exhibiting a positive signal in Toto 50-infected mice were indistinguishable from those of mice infected with TRSB and TR339; however, the virus signal was confined to focal sites, was not associated with infiltrating cells, and did not appear to have spread significantly after 36 hpi (Fig. 6D). H&E-stained sections from Toto 50-infected mice at 6, 8, and 10 days postinfection also were examined. By 6 to 8 days, signs of encephalitis, such as perivascular cuffing, infiltration of mononuclear cells, and focal tissue necrosis, were observed (Fig. 6H).

Consistent with previous reports (29, 61), severe lympholysis in the absence of virus replication was noted in the thymuses of mice infected with TRSB and TR339; however, this pathological change was mild to nonexistent in Toto 50- or mock-infected animals (Fig. 7C to E). Severity of thymic lesions correlated with virulence, as damage in TRSB-infected animals was generally confined to cortical regions, while the thymuses of TR339-infected animals exhibited nearly confluent lympholysis. In addition, apoptosis and/or necrosis, either in the complete absence of virus replication or in areas with occasional ISH-positive cells, was observed in cells of bone marrow, hematopoietic clusters of the liver (Fig. 7G and H), follicular marginal zones of the spleen (Fig. 7I and J), and gut-associated lymphoid tissue. As both TNF-α and corticosterone have been implicated in the induction of apoptosis of hematopoietic and lymphoid cells (12, 17), these characteristic SIRS lesions may be a sensitive indicator of the magnitude of the host response to infection with Sindbis virus.

Treatment of mice with LPS. High-dose LPS treatment of mice causes mortality due to massive induction of proinflammatory cytokines such as TNF-α, IFN-γ, IL-6, and IL-1β (reviewed in reference 2). LPS treatment has been used as a model of SIRS in experimental animal models (reviewed in reference 10). TNF-α has been directly implicated in mortality due to shock, while IFN-γ appears to prime cells to the cytotoxic effects of TNF-α (6, 16) and to increase induction of TNF-α (7). Major pathophysiological changes associated with induction of TNF-α or administration of TNF-α or LPS to adult animals include tachypnea; hypotension; blood acidosis; diminished cardiac output; focal hemorrhage in the lungs, adrenal glands, and pancreas; frank necrosis of the bowel associated with polymorphonuclear cell infiltration and focal loss of epithelium; tubular necrosis of the kidneys; occlusion of pulmonary arteries by polymorphonuclear cells; disseminated intravascular coagulation; apoptosis of thymocytes, bone marrow cells, and splenocytes; and disruption of adipocyte metabolism (58, 59).

To determine the relationship of pathology associated with the LPS-induced SIRS model to that found in TR339-infected neonatal mice, mice were treated with lethal doses of LPS and then H&E-stained tissue sections and cytokine and stress mediator profiles were evaluated. Virtually all of the mice that succumbed to the LPS treatment did so prior to 30 hpi (data not shown). Similar to virulent Sindbis virus-infected mice, LPS-treated neonatal mice exhibited cellular changes morphologically consistent with apoptosis in the thymus, bone marrow, spleen, gut-associated lymphoid tissue, and hematopoietic clusters in the liver. Thymocyte damage was first evident at 4 hpi, becoming severe by 20 hpi. However, lympholysis was frequently confined to cortical regions, as opposed to the confluent lympholysis observed with TR339-infected mice after 48 hpi (Fig. 7F). Other similarities between virus-infected and LPS-treated mice included an increase in condensed and fragmented cell nuclei in the brain and a marked diminution of subcutaneous fat (data not shown). However, frank necrosis of the bowel, loss of intestinal epithelium, and infiltration of mononuclear cells into the intestinal mucosa, submucosa, and lungs, as described for adult animals treated with LPS, were not found in neonatal mice.

Cytokine induction in response to LPS treatment exhibited both quantitative and qualitative differences from the response to virus infection. TNF-α and IL-6 were induced by 2 hpi and reached peak levels greater than 10-fold and 5-fold higher than in TR339-infected mice, respectively (Fig. 8A and B). Levels of both cytokines returned to the baseline between 8 and 20 hpi

magnification, ×100). Dark staining of keratinized epithelium was present in mock-infected animals and is not a consequence of virus replication. (E) H&E-stained section of skeletal muscle from a TR339-infected mouse sacrificed at 60 hpi. The arrow indicates condensed nuclei of muscle cells (original magnification, ×400). (F) ISH of a midsagittal section through the head of a TR339-infected mouse sacrificed at 60 hpi (original magnification, ×100). The arrow indicates the focus of the ISH signal over intact cells with neuronal morphology. (G) H&E-stained adjacent serial section from the area pictured in panel F. The arrow indicates the area of virus replication identified by ISH (original magnification, ×200). (H) H&E-stained section from the brain of a Toto 50-infected mouse 8 days postinfection showing perivascular cuffing and infiltration of mononuclear cells (original magnification, ×400).

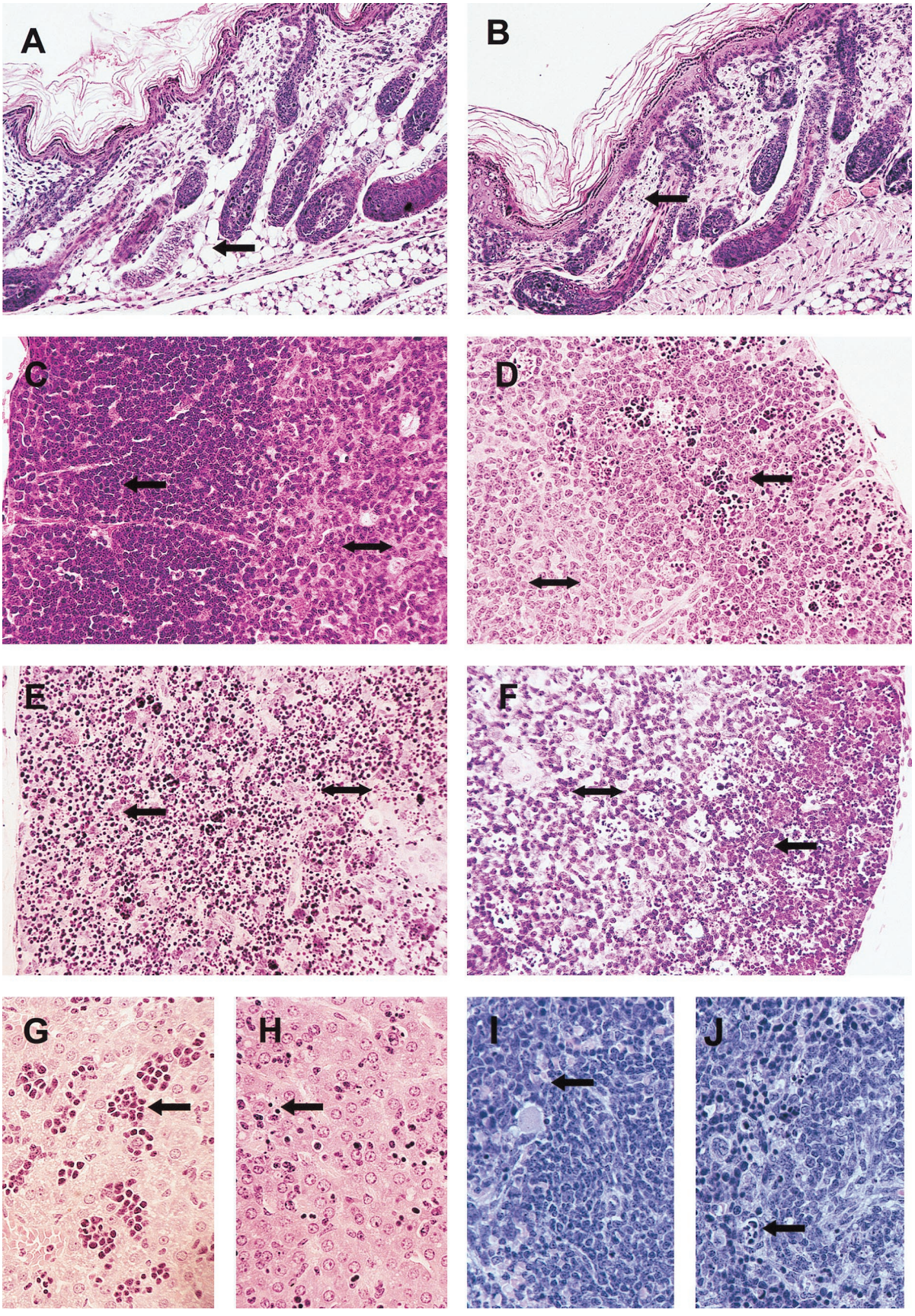

FIG. 7. Histopathological analysis of virus-infected and LPS-treated neonatal mice. (A) Skin of a Toto 50-infected mouse sacrificed at 48 hpi which was indistinguishable from that of mock-infected controls (the arrow indicates subcutaneous fat deposits) (original magnification, ×200). (B) Analogous section from a TR339-infected mouse sacrificed at 48 hpi (the arrow indicates apoptotic and/or necrotic cells in the dermis of the skin) (original magnification, ×200). (C to F) Arrows indicate the thymus cortex, and double arrows indicate the medulla. (C) Thymus from a Toto 50-infected mouse sacrificed at 48 hpi (original magnification, ×400).

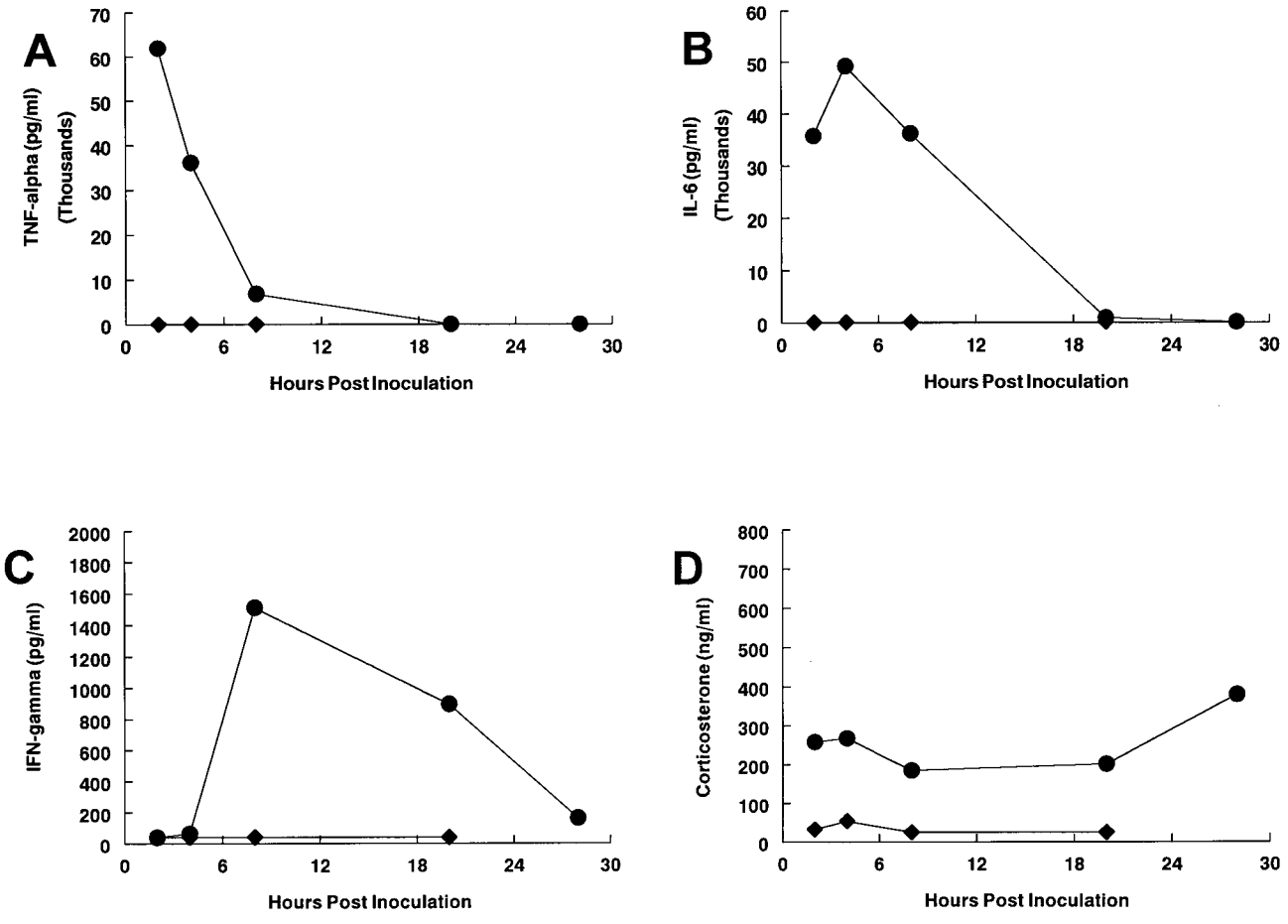

FIG. 8. TNF-α, IFN-γ, IL-6, and corticosterone levels in pooled sera of LPS-treated neonatal mice. TNF-α (A), IL-6 (B), IFN-γ (C), and corticosterone (D) levels in pooled sera from 5 to 10 LPS-treated (●) and mock-treated (◆) neonatal mice are shown.

(prior to the time of death of most animals), in contrast to those of virus-infected mice, which exhibited elevated TNF-α at all times after 12 hpi. In LPS-treated mice, IFN-γ levels rose after 4 hpi, peaking at levels similar to those found in TR339-infected mice (Fig. 8C), while corticosterone levels increased by 2 hpi and remained elevated through 28 hpi (Fig. 8D). In contrast to those of virus-infected mice, IFN-α/β levels did not rise significantly (data not shown).

DISCUSSION

These studies have utilized a genetic approach to determine if the shock-like induction of TNF-α and corticosterone that is characteristic of TRSB infection (61, 63) is (i) an anomalous manifestation of cell-adaptive mutations in this laboratory strain of Sindbis virus or (ii) a previously unrecognized pathology reflective of Sindbis virus strains closer to the native Sindbis virus sequence. To test this hypothesis, the pathogenesis of TRSB was compared with that of TR339, a virus representing the consensus sequence of Sindbis virus AR339 strains. In addition, TRSB pathogenesis was compared to that of Toto 50, a virus with even greater divergence from the consensus sequence.

TRSB infection was characterized by disseminated virus replication in skeletal muscle and fibroblast-connective tissue, followed by invasion of and widespread replication in the central nervous system. Virus replication resulted in induction of high levels of TNF-α, IFN-γ, IFN-α/β, IL-6, and corticosterone in serum, reminiscent of cytokine induction during LPS-induced shock or gram-negative bacterial sepsis (reviewed in reference 2), two causes of SIRS (1, 5). Reduction of the divergence from the consensus sequence led to a SIRS disease even more intense than that caused by TRSB. The Sindbis virus AR339 consensus sequence virus, TR339, produced higher titers in serum, spread more rapidly within the mouse, and resulted in the induction of higher levels of proinflammatory cytokines that correlated with significantly reduced survival time.

(D) Thymus from a TRSB-infected mouse sacrificed at 60 hpi (original magnification, ×400). (E) Thymus from a TR339-infected mouse sacrificed at 60 hpi (original magnification, ×400). (F) Thymus from an LPS-treated mouse sacrificed at 28 hpi (original magnification, ×400). (G) Section through the liver of a mock-infected mouse sacrificed at 60 hpi. The arrow indicates a cluster of hematopoietic cells (original magnification, ×400). (H) Analogous section from a TR339-infected mouse sacrificed at 60 hpi. The arrow indicates the condensed nucleus of a hematopoietic cell (original magnification, ×400). (I) Spleen section from a mock-infected mouse sacrificed at 48 hpi. The arrow indicates the follicle marginal zone (original magnification, ×400). (J) Analogous section from a TR339-infected mouse sacrificed at 48 hpi. The arrow indicates condensed and fragmented nuclei in the marginal zone (original magnification, ×400).

Conversely, increased divergence from the consensus sequence diminished the SIRS disease signs and led to encephalitic pathology. The extensively divergent Toto 50 produced the lowest virus titers, limited cytokine induction, and signs of encephalitis with little pathological evidence of SIRS. This was correlated with extended survival time and reduced mortality relative to those obtained with TRSB.

Virulence differences between TRSB and TR339 were mapped to a single amino acid polymorphism at position 1 of the E2 structural glycoprotein (Ser in TR339, Arg in TRSB). The E2 Arg at position 1 conferred a large increase in binding to BHK cells and to a number of other cultured cell types. This binding was previously shown to be dependent upon cell surface HS (18, 19). Likewise, Toto 50 bound to BHK cells three- to fivefold more efficiently than did TRSB. This virus contains a mutation (Glu to Lys at E2 position 70) which confers attachment to HS (18, 19). Hence, the presence of mutations that confer HS-dependent attachment to cells is correlated with attenuation of the SIRS disease in neonatal mice, most likely arising from reduced rates and extents of virus replication within infected mice. However, the severely attenuated phenotype of Toto 50 likely results not only from the E2 position 70 Lys mutation but also from other mutations at loci in E1, E2, and the 5′ NTR previously shown to affect virulence in mice.

Cytokine profiles and induced pathology in virus-infected and LPS-treated mice. The cytokine and stress mediator profiles observed in these and related studies (61, 63) suggest a connection between the early host response to Sindbis virus infection and mouse mortality. In studies in which proinflammatory cytokine responses to Sindbis virus infection have been measured by quantitative techniques, increased peak levels of cytokines in serum have always correlated with increased mortality and/or decreased AST (48, 62, 63). In addition, the levels of TNF-α present in sera of TR339- and TRSB-infected mice are similar to those reported in SIRS models such as fatal LPS treatment of adult mice and with fatal gram-negative sepsis (4, 25, 50, 60). However, in contrast to transient TNF-α production in LPS-induced shock, mice infected with highly virulent Sindbis virus strains exhibited elevated levels of TNF-α that persisted until death. Sustained levels of TNF-α are closely correlated with mortality in human sepsis studies (4).

Characteristic histological signs of LPS- or TNF-α-mediated (SIRS) pathology, i.e., thymic involution, apoptosis in the spleen and bone marrow, destruction of hematopoietic cells in the liver, and depletion of adipocytes were present in TRSB-infected mice in the absence of colocalized virus replication. Consistent with higher inflammatory cytokine levels in TR339-infected mice, all of these signs were more severe. Such pathological changes in TR339-infected mice were similar to or more severe than in mice treated with lethal doses of LPS. In contrast, TNF-α and IL-6 induction in LPS-treated neonates was significantly greater than that observed with TR339 infection but of shorter duration, consistent with reported differences between LPS-treated and septic animals (2). Together, these results provide a strong circumstantial case for involvement of SIRS in disease induced by virulent Sindbis virus.

There also may be significant differences between conventional shock-sepsis models and the disease produced in Sindbis virus-infected neonatal mice. Murine cytomegalovirus infection of mice produces a qualitatively different inflammatory response than LPS-induced shock in that murine cytomegalovirus induces corticosterone by an IL-6-dependent pathway while LPS-induced corticosterone is IL-6 independent (46). In the Sindbis virus model, we have been unable to reliably detect higher levels of IL-1β in infected animals compared to mock-infected controls (data not shown). This result, in combination with the induction of high levels of IFN-α/β only in virus-infected mice, indicates possible qualitative differences between SIRS induced by LPS and that induced by Sindbis virus.

Likewise, as few studies have evaluated in detail the effect of high levels of proinflammatory cytokines on neonatal animals, there may be significant differences in their responses compared to those of adults. Consistent with the results described in this report, previous treatment of neonatal mice with recombinant TNF-α failed to produce the characteristic lung and gastrointestinal tract pathology associated with high levels of TNF-α in adult animals (9). In addition, limited inflammatory cell infiltrates in LPS-treated and Sindbis virus-infected neonatal mice may reflect defects in polymorphonuclear cell activation, chemotaxis, and production of several cytokines documented for neonatal animals (21, 26, 30, 32).

Cytokine-mediated cell damage. We observed condensed and fragmented cell nuclei in many peripheral tissues of TRSB- and TR339-infected mice, both in association with and in the absence of virus replication. Similar, although much less extensive, pathological changes were observed in the brains of LPS-treated and virus-infected mice. Induction of proinflammatory cytokines has been associated with potentiation of both apoptotic and necrotic tissue injury in animal models of viral and other diseases (8, 33, 34, 39, 42, 45, 49, 56, 60). Apoptosis has been documented in the intestines, livers, lungs, fat, thymuses, and endothelial cells of LPS- and TNF-α-treated mice (3, 11) and in one study was causally linked to mortality (11). In neonatal infections, the blood-brain barrier may be more permeable (53) and permeability can be enhanced by circulating cytokines (27, 41). Hence, cells in the neonatal central nervous system may be subject to effects of host factors secreted into the blood, contributing to pathological changes observed with Sindbis virus infection or LPS treatment.

Moreover, virus infection of cells may alter responses to cytokines. In vitro and in vivo sensitivity to TNF-α-mediated cytotoxicity is greatly enhanced by inhibitors of cellular transcription and/or translation (3, 22, 33, 54), and infection with several viruses sensitizes cells to the cytotoxic effects of TNF-α (20, 37, 44). A primary effect of Sindbis virus infection is repression of host cell transcription, DNA replication, and translation (55). It is possible that Sindbis virus-infected cells have altered sensitivity to the effects of TNF-α or other circulating host factors.

Proximal cause of death due to Sindbis virus infection. A particularly complicating factor in these neonatal mouse studies may be the relatively unrestrained replication of virulent Sindbis virus, leading to extensive damage to virus-infected cells and extensive damage to cells as a consequence of proinflammatory cytokine induction. Fatal outcome may reflect the cooperative activities of several pathologic mechanisms, any one of which could result in mortality if allowed to manifest fully. However, these studies suggest that SIRS is a major contributing factor in virulent Sindbis virus disease in which disseminated infection results in multiple pathological conditions and rapid death. Moreover, the SIRS component of Sindbis virus-induced disease in neonatal animals is observed only with strains closely reflecting the consensus sequence of the virus and not with strains extensively adapted to cell culture replication. This underscores the necessity of the identification and elimination of the effects of tissue culture adaptation on viral strains used in animal models of disease.

ACKNOWLEDGMENTS

This work was supported by Public Health Service-NIH grants AI22186 and CA41268. W.B.K. was supported by an NIH predoctoral

traineeship (T32 AI07419) and by the U.S. Army Research Office (DAAH04-95-1-0224).

REFERENCES

1. **American College of Chest Physicians/Society of Critical Care Medicine.** 1992. Definitions for sepsis and organ failure and guidelines for the use of innovative therapies in sepsis. Crit. Care Med. **1992:**864–874.
2. **Billiau, A., and F. Vandekerckhove.** 1991. Cytokines and their interactions with other inflammatory mediators in the pathogenesis of sepsis and septic shock. Eur. J. Clin. Investig. **21:**559–573.
3. **Bohlinger, I., M. Leist, F. Gantner, S. Angelmuller, G. Tiegs, and A. Wendel.** 1996. DNA fragmentation in mouse organs during endotoxic shock. Am. J. Pathol. **149:**1381–1393.
4. **Calandra, T., J.-D. Baumgartner, G. E. Grau, M.-M. Wu, P.-H. Lambert, J. Schellekens, J. Verhoef, M. P. Glauser, and The Swiss-Dutch J5 Immunoglobulin Study Group.** 1990. Prognostic values of tumor necrosis factor/cachectin, interleukin-1, interferon-alpha, and interferon-gamma in the serum of patients with septic shock. J. Infect. Dis. **161:**982–987.
5. **Davies, M. G., and P.-O. Hagen.** 1997. Systemic inflammatory response syndrome. Br. J. Surg. **84:**920–935.
6. **Dealtry, G. B., M. S. Naylor, W. Fiers, and F. R. Balkwill.** 1987. DNA fragmentation and cytotoxicity caused by tumor necrosis factor is enhanced by interferon-gamma. Eur. J. Immunol. **17:**689–693.
7. **Doherty, G. M., J. R. Lange, H. N. Langstein, H. R. Alexander, C. M. Buresh, and J. A. Norton.** 1992. Evidence for IFN-gamma as a mediator of the lethality of endotoxin and tumor necrosis factor-alpha. J. Immunol. **149:**1666–1670.
8. **Grau, G., L. F. Fajardo, P.-F. Piguet, B. Allet, P.-H. Lambert, and P. Vassalli.** 1987. Tumor necrosis factor (cachectin) as an essential mediator in murine cerebral malaria. Science **237:**210–213.
9. **Gresser, I., D. Woodrow, J. Moss, C. Maury, J. Tavernier, and W. Fiers.** 1987. Toxic effects of recombinant tumor necrosis factor in suckling mice. Am. J. Pathol. **128:**13–18.
10. **Gutierrez-Ramos, J. C., and H. Bluethmann.** 1997. Molecules and mechanisms operating in septic shock: lessons from knockout mice. Immunol. Today **18:**329–334.
11. **Haimovitzfriedman, A., C. Cordoncardo, S. Bayoumy, M. Garzotto, M. McLoughlin, R. Gallily, C. K. Edwards, E. H. Schuchman, Z. Fuks, and R. Kolesnick.** 1997. Lipopolysaccharide induces disseminated endothelial apoptosis requiring ceramide generation. J. Exp. Med. **186:**1831–1841.
12. **Hernandez-Caselles, T., and O. Stutman.** 1993. Immune functions of tumor necrosis factor. I. Tumor necrosis factor induces apoptosis of mouse thymocytes and can also stimulate or inhibit IL-6-induced proliferation depending on the type of mitogenic costimulation. J. Immunol. **151:**3999–4012.
13. **Jan, J. T., A. P. Byrnes, and D. E. Griffin.** 1999. Characterization of a Chinese hamster ovary cell line developed by retroviral insertional mutagenesis that is resistant to Sindbis virus infection. J. Virol. **73:**4919–4924.
14. **Johnson, R. T.** 1965. Virus invasion of the central nervous system: a study of Sindbis virus infection of the mouse using fluorescent antibody. Am. J. Pathol. **46:**929–943.
15. **Johnson, R. T., H. F. McFarland, and S. E. Levy.** 1972. Age-dependent resistance to viral encephalitis: studies of infections due to Sindbis virus in mice. J. Infect. Dis. **125:**257–262.
16. **Kato, Y., A. Morikawa, T. Sugiyama, N. Koide, G.-Z. Jiang, T. Lwin, T. Yoshida, and T. Yokochi.** 1997. Augmentation of lipopolysaccharide-induced thymocyte apoptosis by interferon-gamma. Cell. Immunol. **177:**103–108.
17. **Kato, Y., A. Morikawa, T. Sugiyama, N. Koide, G.-Z. Jiang, T. Takahashi, and T. Yokochi.** 1995. Role of tumor necrosis factor-alpha and glucocorticoid on lipopolysaccharide (LPS)-induced apoptosis of thymocytes. FEMS Immunol. Med. Microbiol. **12:**195–204.
18. **Klimstra, W. B., H. W. Heidner, and R. E. Johnston.** 1999. The furin protease cleavage recognition sequence of Sindbis virus PE2 can mediate virion attachment to cell surface heparan sulfate. J. Virol. **73:**6299–6306.
19. **Klimstra, W. B., K. D. Ryman, and R. E. Johnston.** 1998. Adaptation of Sindbis virus to BHK cells selects for use of heparan sulfate as an attachment receptor. J. Virol. **72:**7357–7366.
20. **Koff, W. C., and A. V. Fann.** 1986. Human tumor necrosis factor-alpha kills herpesvirus-infected but not normal cells. Lymphokine Res. **5:**215–221.
21. **Krause, P. J., J. Kristie, W. P. Wang, L. Eisenfeld, V. C. Herson, E. G. Maderazo, K. Jozaki, and D. L. Kreutzer.** 1987. Pentoxifylline enhancement of defective neutrophil function and host defense in neonatal mice. Am. J. Pathol. **129:**217–222.
22. **Laster, S. M., J. G. Wood, and L. R. Gooding.** 1988. Tumor necrosis factor can induce both apoptotic and necrotic forms of cell lysis. J. Immunol. **141:**2629–2634.
23. **Levine, B., J. E. Goldman, H. H. Jiang, D. E. Griffin, and J. M. Hardwick.** 1996. Bcl-2 protects mice against fatal alphavirus encephalitis. Proc. Natl. Acad. Sci. USA **93:**4810–4815.
24. **Levine, B., and D. E. Griffin.** 1993. Molecular analysis of neurovirulent strains of Sindbis virus that evolve during persistent infection of *scid* mice. J. Virol. **67:**6872–6875.
25. **Li, P., H. Allen, S. Banerjee, S. Franklin, L. Herzog, C. Johnston, J. McDowell, M. Paskind, L. Rodman, J. Salfield, E. Towne, D. Tracey, S. Wardwell, F.-Y. Wei, W. Wong, R. Kamen, and T. Seshardi.** 1995. Mice deficient in IL-1B-converting enzyme are defective in production of mature IL-1B and resistant to endotoxic shock. Cell **80:**401–411.
26. **Liechty, K. W., K. R. Schibler, R. K. Ohls, S. L. Perkins, and R. D. Christensen.** 1993. The failure of newborn mice infected with Escherichia coli to accelerate neutrophil production correlates with their failure to increase transcripts for granulocyte-colony stimulating factor and interleukin-6. Biol. Neonate **64:**331–340.
27. **Lustig, S., H. D. Danenberg, Y. Kafri, D. Kobiler, and D. Ben-Nathan.** 1992. Viral neuroinvasion and encephalitis induced by lipopolysaccharide and its mediators. J. Exp. Med. **176:**707–712.
28. **Lustig, S., A. C. Jackson, C. S. Hahn, D. E. Griffin, E. G. Strauss, and J. H. Strauss.** 1988. Molecular basis of Sindbis virus neurovirulence in mice. J. Virol. **62:**2329–2336.
29. **Mahlerbe, H., M. Strickland-Chomley, and A. L. Jackson.** 1963. Sindbis virus infection in man: report of a case with recovery of virus from skin lesions. S. Afr. Med. J. **37:**547–552.
30. **Martin, T. R., J. T. Ruzinski, C. B. Wilson, and S. J. Skerrett.** 1995. Effects of endotoxin in the lungs of neonatal rats: age-dependent impairment of the inflammatory response. J. Infect. Dis. **171:**131–144.
31. **McKnight, K. L., D. A. Simpson, S. C. Lin, T. A. Knott, J. M. Polo, D. F. Pence, D. B. Johannsen, H. W. Heidner, N. L. Davis, and R. E. Johnston.** 1996. Deduced consensus sequence of Sindbis virus strain AR339: mutations contained in laboratory strains which affect cell culture and in vivo phenotypes. J. Virol. **70:**1981–1989.
32. **Merry, C., P. Puri, and D. J. Reen.** 1996. Defective neutrophil actin polymerization and chemotaxis in stressed newborns. J. Pediatr. Surg. **31:**481–485.
33. **Morikawa, A., T. Sugiyama, Y. Kato, N. Kiode, G.-Z. Jiang, K. Takahashi, Y. Tamada, and T. Yokochi.** 1996. Apoptotic cell death in the response of D-galactosamine-sensitized mice to lipopolysaccharide as an experimental endotoxic shock model. Infect. Immun. **64:**734–738.
34. **Nagano, I., S. Nakamura, M. Yoshioka, J. Onodera, K. Kogure, and Y. Itoyama.** 1994. Expression of cytokines in brain lesions in subacute sclerosing panencephalitis. Neurology **44:**710–715.
35. **Nava, V. E., A. Rosen, M. A. Veliuona, R. J. Clem, B. Levine, and J. M. Hardwick.** 1997. Sindbis virus induces apoptosis through a caspase-dependent CrmA-sensitive pathway. J. Virol. **72:**452–459.
36. **Nguyen, K. B., and C. A. Biron.** 1999. Synergism for cytokine-mediated disease during concurrent endotoxin and viral challenges: role for NK and T cell IFN-γ production. J. Immunol. **162:**5238–5246.
37. **Ohno, K., T. Nakano, Y. Matsumoto, T. Watari, R. Goitsuka, H. Nakayama, H. Tsujimoto, and A. Hasegawa.** 1993. Apoptosis induced by tumor necrosis factor in cells chronically infected with feline immunodeficiency virus. J. Virol. **67:**2429–2433.
38. **Orange, J. S., and C. A. Biron.** 1996. An absolute and restricted requirement for IL-12 in natural killer cell IFN-gamma production and antiviral defense. J. Immunol. **156:**1138–1142.
39. **Orange, J. S., T. P. Salazar-Mather, S. M. Opal, and C. A. Biron.** 1997. Mechanisms for virus-induced liver disease: tumor necrosis factor-mediated pathology independent of natural killer and T cells during murine cytomegalovirus infection. J. Virol. **71:**9248–9258.
40. **Polo, J. M., and R. E. Johnston.** 1990. Attenuating mutations in glycoproteins E1 and E2 of Sindbis virus produce a highly attenuated strain when combined in vitro. J. Virol. **64:**4438–4444.
41. **Quagliarello, V. J., B. Wispelwey, W. J. J. Long, and W. M. Scheld.** 1991. Recombinant interleukin-1 induces meningitis and blood brain barrier injury in the rat. Characterization and comparison with tumor necrosis factor. J. Clin. Investig. **87:**1360–1366.
42. **Relton, J. K., and N. J. Rothwell.** 1992. Interleukin-1 receptor antagonist inhibits ischemic and excitotoxic neuronal damage in the rat. Brain Res. Bull. **29:**243–246.
43. **Rice, C. M., R. Levis, J. H. Strauss, and H. V. Huang.** 1987. Production of infectious RNA transcripts from Sindbis virus cDNA clones: mapping of lethal mutations, rescue of a temperature-sensitive marker, and in vitro mutagenesis to generate defined mutants. J. Virol. **61:**3809–3819.
44. **Rood, P. A., R. M. Lorence, and K. W. Kelley.** 1990. Serine protease inhibitor abrogation of Newcastle disease virus enhancement of cytolysis by recombinant tumor necrosis factors alpha and beta. J. Natl. Cancer Inst. **82:**213–217.
45. **Ruddle, N. H., C. M. Bergman, K. M. McGrath, E. G. Lingenheld, M. L. Grunnet, and S. J. Padula.** 1990. An antibody to lymphotoxin and tumor necrosis factor prevents transfer of experimental allergic encephalomyelitis. J. Exp. Med. **172:**1193–1200.
46. **Ruzek, M. C., A. H. Miller, S. M. Opal, B. D. Pearce, and C. A. Biron.** 1997. Characterization of early cytokine responses and an IL-6-dependent pathway of endogenous glucocorticoid induction during murine cytomegalovirus infection. J. Exp. Med. **185:**1185–1192.
47. **Ruzek, M. C., B. D. Pearce, A. H. Miller, and C. A. Biron.** 1999. Endogenous glucocorticoids protect against cytokine-mediated lethality during viral infection. J. Immunol. **162:**3527–3533.
48. **Ryman, K. D., and R. E. Johnston.** 1997. Unpublished observations.

49. **Saukkonen, K., S. Sande, C. Cioffe, S. Wolpe, B. Sherry, A. Cerami, and E. Toumanan.** 1990. The role of cytokines in the generation of inflammation and tissue damage in experimental gram-positive meningitis. J. Exp. Med. **171:**439–448.
50. **Shapria, L., W. A. Soskolne, Y. Houri, V. Barak, A. Halabi, and A. Stabholz.** 1996. Protection against endotoxic shock and lipopolysaccharide-induced local inflammation by tetracycline: correlation with inhibition of cytokine secretion. Infect. Immun. **64:**825–828.
51. **Sherman, L. A., and D. E. Griffin.** 1990. Pathogenesis of encephalitis induced in newborn mice by virulent and avirulent strains of Sindbis virus. J. Virol. **64:**2041–2046.
52. **Simpson, D. A., N. L. Davis, S. C. Lin, D. Russell, and R. E. Johnston.** 1996. Complete nucleotide sequence and full-length cDNA clone of S.A.AR86, a South African alphavirus related to Sindbis. Virology **222:**464–469.
53. **Skultetyova, I., D. I. Tokarev, and D. Jezova.** 1993. Albumin content in the developing rat brain in relation to the blood-brain barrier. Endocr. Regul. **27:**209–213.
54. **Slowik, M. R., W. Min, T. Ardito, A. Karsan, M. Kashagarian, and J. S. Pober.** 1997. Evidence that tumor necrosis factor triggers apoptosis in human endothelial cells by interleukin-1-converting enzyme-like protease-dependent and -independent pathways. Lab. Investig. **77:**257–267.
55. **Strauss, J. H., and E. G. Strauss.** 1994. The alphaviruses: gene expression, replication, and evolution. Microbiol. Rev. **58:**491–562.
56. **Talley, A., S. Perry, L. G. Epstein, and H. A. Gelbard.** 1994. TNFa-mediated apoptosis in SK-N-MC neuroblastoma cells: a model for neuronal cell loss in HIV-1-associated dementia. Ann. Neurol. **36:**506–507.
57. **Taylor, R. M., H. S. Hurlbut, T. H. Work, J. R. Kingston, and T. E. Rothingham.** 1955. Sindbis virus: a newly recognized arthropod-transmitted virus. Am. J. Trop. Med. Hyg. **4:**844–862.
58. **Torti, F. M., B. Dieckmann, B. Beutler, A. Cerami, and G. M. Ringold.** 1985. A macrophage factor inhibits adipocyte gene expression: an in vitro model of cachexia. Science **229:**867–869.
59. **Tracey, K. J., B. Beutler, S. F. Lowry, J. Merryweather, S. Wolpe, I. W. Milsark, R. J. Hariri, T. J. Fahey, A. Zentella, J. D. Albert, G. T. Shires, and A. Cerami.** 1986. Shock and tissue injury induced by recombinant human cachectin. Science **234:**470–474.
60. **Tracey, K. J., Y. Fong, D. G. Hesse, K. R. Manogue, A. T. Lee, G. C. Kuo, S. F. Lowry, and A. Cerami.** 1987. Anti cachectin/TNF monoclonal antibodies prevent septic shock during lethal bacteraemia. Nature **330:**662–664.
61. **Trgovcich, J., J. F. Aronson, and R. E. Johnston.** 1996. Fatal Sindbis virus infection of neonatal mice in the absence of encephalitis. Virology **224:**73–83.
62. **Trgovcich, J., and R. E. Johnston.** TNF α, interferon and stress response induction as a function of age-related susceptibility to fatal Sindbis virus infection of mice. Virology, in press.
63. **Trgovcich, J., K. Ryman, P. Extrom, J. C. Eldridge, J. F. Aronson, and R. E. Johnston.** 1997. Sindbis virus infection of neonatal mice results in a severe stress response. Virology **227:**234–238.
64. **Tucker, P. C., E. G. Strauss, R. J. Kuhn, J. H. Strauss, and D. E. Griffin.** 1993. Viral determinants of age-dependent virulence of Sindbis virus for mice. J. Virol. **67:**4605–4610.